Available online at www.sciencedirect.com

ScienceDirect

Advances in Space Research 65 (2020) 745–755

ADVANCES IN SPACE RESEARCH (a COSPAR publication)

www.elsevier.com/locate/asr

RATAN-600 and RadioAstron reveal the neutrino-associated blazar TXS 0506+056 as a typical variable AGN

Yu.A. Kovalev [a,*], N.S. Kardashev [a,†], Y.Y. Kovalev [a,b,c], K.V. Sokolovsky [a,d,e], P.A. Voitsik [a], P.G. Edwards [f], A.V. Popkov [b,a], G.V. Zhekanis [g], Yu.V. Sotnikova [g], N.A. Nizhelsky [g], P.G. Tsybulev [g], A.K. Erkenov [g], N.N. Bursov [g]

[a] *Astro Space Center of Lebedev Physical Institute, Profsoyuznaya St. 84/32, 117997 Moscow, Russia*
[b] *Moscow Institute of Physics and Technology, Dolgoprudny, Institutsky per., 9, Moscow Region 141700, Russia*
[c] *Max-Planck-Institut für Radioastronomie, Auf dem Hügel 69, 53121 Bonn, Germany*
[d] *Department of Physics and Astronomy, Michigan State University, East Lansing, MI 48824, USA*
[e] *Sternberg Astronomical Institute, Moscow State University, Universitetskii pr. 13, 119992 Moscow, Russia*
[f] *Australia Telescope National Facility, CSIRO, PO Box 76, Epping, NSW 1710, Australia*
[g] *Special Astrophysical Observatory, Russian Academy of Sciences, Nizhnii Arkhyz 369167, Russia*

Received 22 December 2018; received in revised form 23 April 2019; accepted 29 April 2019
Available online 9 May 2019

Abstract

The possible association with the high-energy neutrino event IceCube-170922A has sparked interest in the blazar TXS 0506+056. We present 72 instantaneous 1–22 GHz spectra measured over the past 20 years with the RATAN-600 telescope and compare them with the results of observations of 700 variable Active Galactic Nuclei (AGN) studied within the same program. The recent radio flare of TXS 0506+056 started from a minimum in 2013 and reached its first peak in December 2017 and a second peak in May-June 2018. This was the third strong radio flare in this source since 1997. The spectrum remains nearly flat during the flares. The spectral shape and variability pattern observed in TXS 0506+056 are typical for variable AGN. *RadioAstron* Space VLBI observations in 2013–2015 did not detect TXS 0506+056 on space-ground baselines of more than 9 Earth diameters. However, an observation on 23 September 2015 resulted in the detection of interferometric signal on 6 Earth diameter baselines at 18 cm close to the detection limit. We consider the possibility that TXS 0506+056 and other AGN may accelerate relativistic protons more efficiently than electrons. Relativistic protons are necessary to produce both the high-energy neutrinos observed in the IceCube Observatory and the high AGN brightness temperatures implied by the *RadioAstron* detection. They may also provide the main contribution to the observed synchrotron radiation of parsec-scale AGN jets. This supports the suggestion that relativistic protons may play a much more important part in extragalactic astrophysics than earlier anticipated.

Keywords: Active galactic nuclei; Radio astronomy; Neutrino; Quasars: individual: TXS 0506+056

1. Introduction

The first high-energy neutrino associated with an extragalactic object was detected from the direction of TXS 0506+056 on September 22, 2017 (Aartsen et al., 2018a) by the IceCube observatory at the South Pole (Aartsen et al., 2017). Analysis of earlier IceCube data revealed an additional 13 ± 5 lower-energy neutrino events recorded between September 2014 and March 2015 that could be attributed to TXS 0506+056 (Aartsen et al., 2018b). The source is a jet-emission–dominated active galaxy (a blazar) at the redshift of $z = 0.3365$ (Paiano

* Corresponding author.
E-mail address: ykovalev@asc.rssi.ru (Y.A. Kovalev).
† Deceased on 3 August 2019.

https://doi.org/10.1016/j.asr.2019.04.034
0273-1177/

et al., 2018). It is uncertain which blazar sub-type this source belongs to: Véron-Cetty and Véron (2010) list it as a BL Lac type object while Padovani et al. (2019) suggest it is actually a quasar. It is the first high-confidence association of a PeV-energy neutrino with a source and only the third associated astrophysical neutrino source after the Sun and the supernova SN 1987A. This association supports the long-standing assumption that relativistic jets in active galactic nuclei are responsible for the production of ultra high-energy cosmic rays and the extraterrestrial diffuse flux of high-energy neutrinos (Mannheim, 1995; Halzen, 2016; Mészáros, 2017). Ansoldi et al. (2018), Aartsen et al. (2018a) discuss the high-energy and multi-wavelength properties of TXS 0506+056.

The radio source TXS 0506+056 was catalogued in the Ohio Survey (Ehman et al., 1970) as OG 012, but first came to prominence with the RATAN-600 (see Section 2) discovery of day-scale variability by Gorshkov and Konnikova (1996). It was studied as one of the 5-GHz VSOP Survey sources by the first space VLBI mission with the HALCA satellite (Hirabayashi et al., 2000). No signal was detected on space-ground baselines. The VSOP AGN Survey catalog lists a correlated flux density of 0.25 Jy on the longest VLBA baselines (Dodson et al., 2008).

2. RATAN-600 1–22 GHz spectrum monitoring

RATAN-600 is the 600 m ring radio telescope in Zelenchukskaya, Russia (Korolkov and Pariiskii, 1979). It is operated mostly in transit mode for measuring broad-band spectra.

The 1–22 GHz instantaneous spectrum of TXS 0506 +056 was first obtained by our team in 1997. The spectrum was flat, with flux densities of about 0.5 Jy (Fig. 2 in Kovalev et al., 2000b). Along with another 213 VSOP 5-GHz survey sources, TXS 0506+056 was regularly monitored with RATAN-600 by Kovalev et al. (2000a). Over the following years this research was continued in an expanded monitoring program for about 700 AGNs in order to study the long term variability of their instantaneous 1–22 GHz spectra. Observations of about 2000 AGN were also carried out in 2000–2003 in order to study the shapes and types of their spectra (Kovalev et al., 2004). To date, 1–22 GHz spectra have been obtained at 4–6 frequencies for TXS 0506+056 at 72 epochs between 1997 and 2018. This includes spectra at epochs 2017.69, 2017.72, 2017.73 and 2017.74 corresponding to the dates 2017 September, 6, 14, 16 and 22, where the last is the date of the high energy neutrino detection. The data reduction procedure, main list of monitored sources and results of observations and model analysis have been presented by Kovalev et al. (1999, 2000a, 2002a). The additional RATAN-600 1–22 GHz spectra of TXS 0506+056 obtained between 2006 and 2017 are reported by Mingaliev et al. (2014).

The multi-messenger observational data for this object have been recently published by Aartsen et al. (2018b). Long-term observations of AGN have been carried out by Richards et al. (2011), Aller et al. (1985), Angelakis et al. (2019), Teräsranta et al. (2005), Ackermann et al. (2015).

The main results of the 20-year spectral study of TXS 0506+056 are in agreement with the conclusions in Kovalev et al. (2000a, 2002a, 2004). In comparison with the property of the studied objects they can be summarised as follows.

TXS 0506+056 is a typical variable AGN (see Fig. 1). The instantaneous spectra have been measured for several minutes at all wavelengths: 1.38, 2.7, 3.9 (3.7), 6.3, 6.4, 7.6, 13 and 31 (24) cm. The corresponded frequencies are 21.7, 11.2, 7.7 (8.1), 4.8, 4.7, 3.9, 2.3, 0.96 (1.25) GHz. The spectra of 2600 AGN (see examples in Figs. 1–4) can be divided into 5 main types (Kovalev et al., 2004):

1. with a maximum or minimum (11%),
2. inverted ($\alpha > +0.1$, where $F \propto \nu^{\alpha}$ – 10%),
3. super-flat ($|\alpha| \leqslant 0.1$ at 3 or more of the highest frequencies, like TXS 0506+056 spectra, – 20%),
4. steep ($\alpha < -0.1$, – 41%), and
5. variable (between any of types 1–4 above, – 14%).

A radio spectrum is called "flat" if its spectral index $\alpha > -0.5$. As can be seen in Fig. 1, the spectra of TXS 0506+056 on some occasions differs from super-flat (see, e.g., the boxes for 1999–2000, 2003–2004, 2009–2010, 2017–2018). Continuum spectra of AGN covering such a wide frequency range can be explained by a sum of two major contributions. We call them the high (HFC) and low (LFC) frequency spectral component. See, e.g., Fig. 1 in Kovalev et al. (2002a) and the spectra for 2230 +11 in Fig. 2. The HFC is associated with the parsec-scale jet and dominates at frequencies of several GHz and above. Its properties are determined by the partly opaque and variable base of the jet. The LFC represents an optically thin synchrotron radiation of extended structures up to kiloparsec scales and has a peak frequency much less than 1 GHz due to its characteristic size (Slish, 1963). The correlated flux density measured by VLBI should correspond to the compact HFC emission (Kovalev et al., 2005).

3. RadioAstron space VLBI observations

RadioAstron (Kardashev et al., 2013) is a space VLBI mission combining a 10 m orbiting radio telescope with a ground-based array to perform ultra-high angular resolution imaging (e.g. Gómez et al., 2016; Giovannini et al., 2018) and visibility-tracking (e.g. Kovalev et al., 2016; Pilipenko et al., 2018; Kutkin et al., 2018) observations in the 1.7, 4.8 and 22 GHz bands. Thanks to its long space-ground baselines of up to 28 Earth diameters, *RadioAstron* can directly measure brightness temperatures up to 10^{16} K.

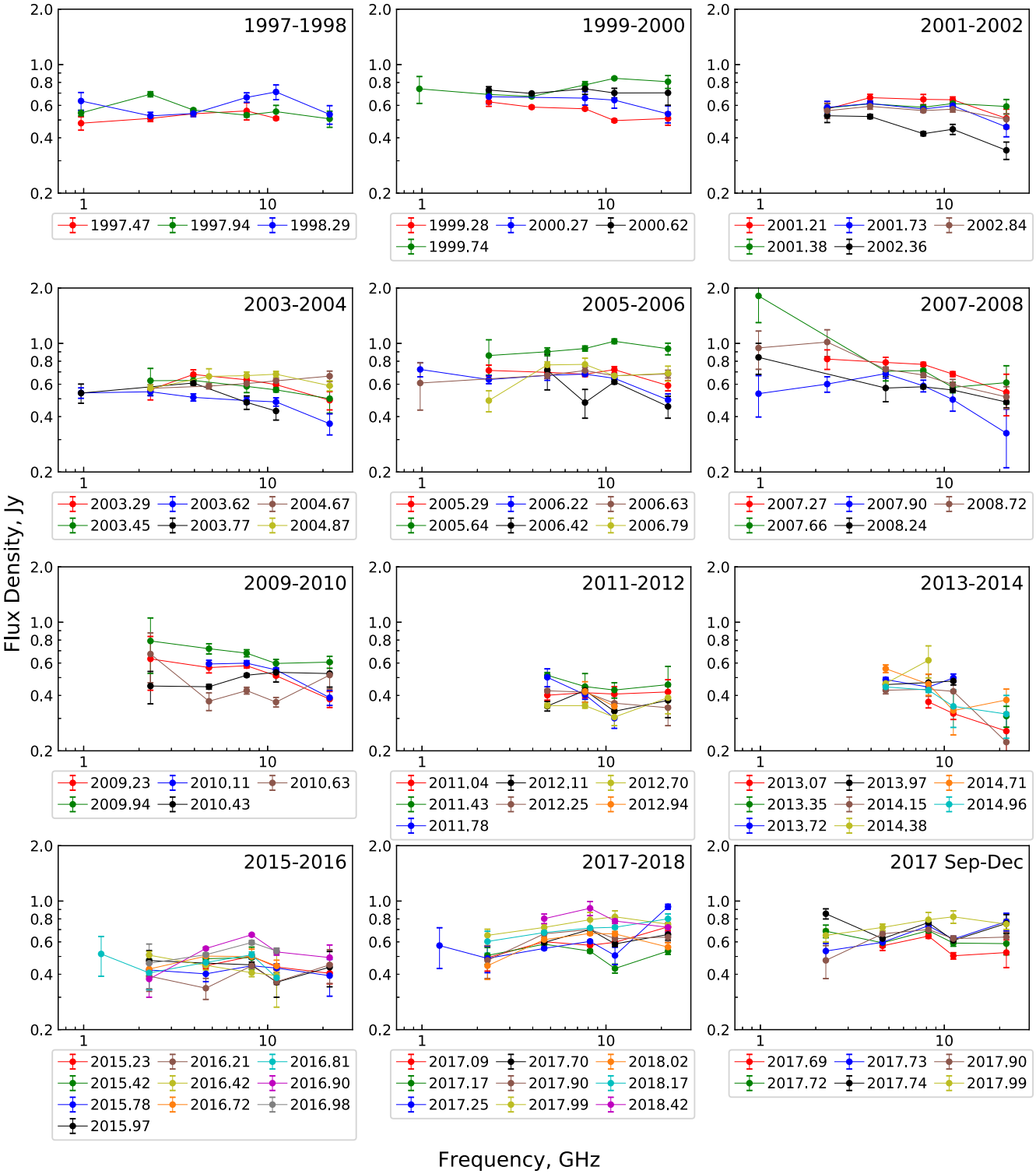

Fig. 1. The RATAN-600 instantaneous 1–22 GHz spectra of TXS 0506+056 for 72 epochs between 1997 June and 2018 June. The date of the high energy neutrino detection, 22 September 2017, is labeled as 2017.74.

TXS 0506+056 was observed as part of the *RadioAstron* AGN survey (Kovalev et al., this issue) between 2013 and 2015. The observations were conducted at 1.7 and 4.8 GHz on projected baselines between 6 and 17 Earth diameters, and resulted in non-detections according to the standard AGN survey criteria. We note these non-detections occurred before the PeV neutrino detection. A complete list of observations is presented in Table 1. All observations were processed with the ASC correlator (Likhachev et al., 2017) in Moscow and

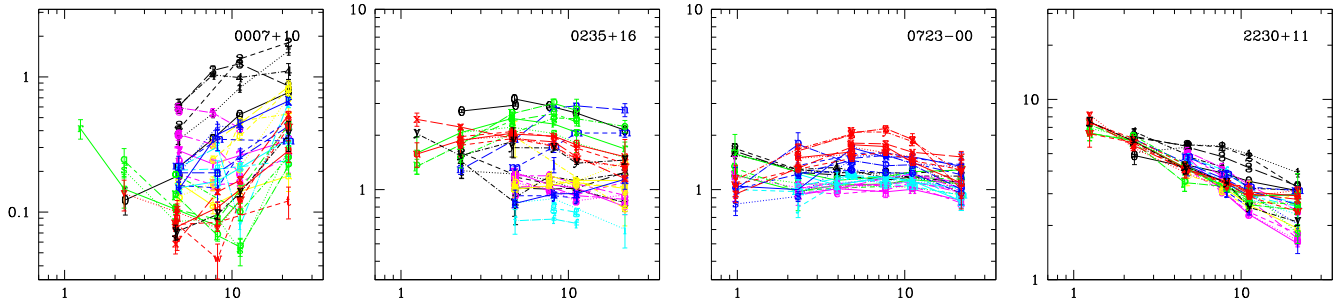

Fig. 2. Examples of the broad-band spectral variability in 1997–2009 for 0723−00 and in 2009–2017 for other 3 AGN from our survey in order to compare with the spectra of TXS 0506+056 on Fig. 1. The classifications of the variable spectra are: variable (0723−00 – between types 1 and 3, 0007+10, 0235 +16), and steep (2230+11) – see Fig. 4 for details. The flux density in Jy is plotted against the frequency in GHz. The names of the objects in boxes are given to the epoch B 1950.0. Spectra observed at different observing epochs are shown by different colors. (For interpretation of the references to color in this figure legend, the reader is referred to the web version of this article.)

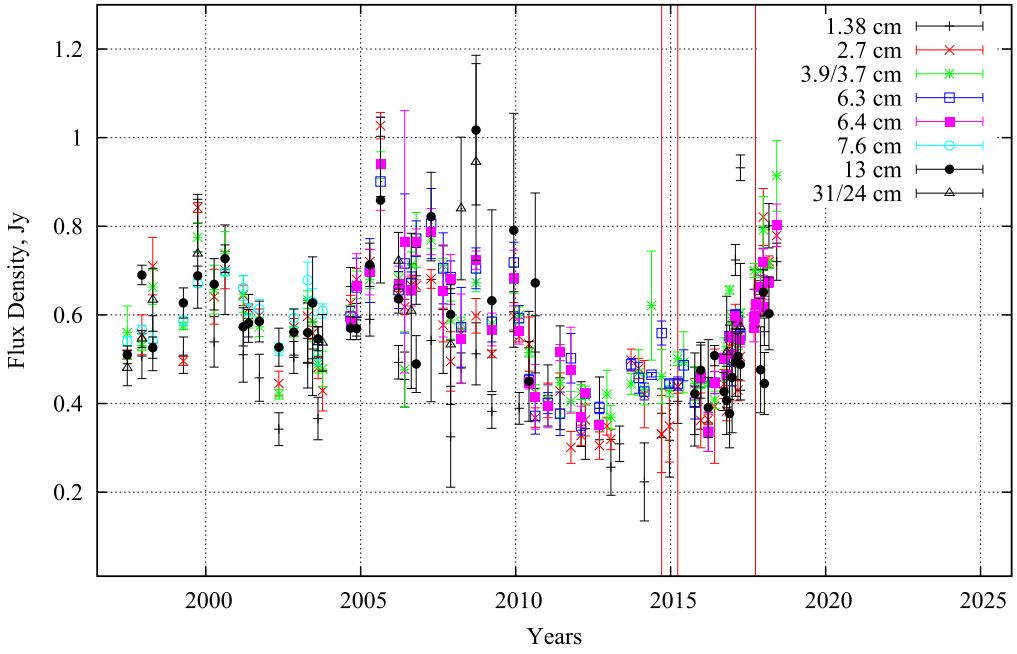

Fig. 3. The RATAN-600 light-curve of TXS 0506+056. The red vertical lines mark the date of IceCube-170922A neutrino main event on 2017 September 22 as well as the earlier low-energy neutrino evens between 2014 September and 2015 March (Aartsen et al., 2018b). (For interpretation of the references to color in this figure legend, the reader is referred to the web version of this article.)

fringe-searched (“signal-searched”) with PIMA (Petrov et al., 2011).

Deep analysis of the observation conducted on September 23, 2015 reveals one 1.7 GHz scan on the projected *RadioAstron* Space Radio Telescope – Medicina 32 m baseline of 414 Mλ (5.9 Earth diameters) that shows a signal-to-noise ratio of 5.5 in a narrow residual delay-rate window (Fig. 5). The fringe (signal) amplitude corresponds to a probability of false detection of less than 5% and the position of the signal near zero delay, rate and acceleration further suggests that this detection is real. The other three scans of the same length (15 min) in this experiment resulted in no signal detections. This may be interpreted as an indication that the correlated flux density in this experiment was just below the detection limit. Using system temperatures and gains for the Space Radio Telescope (Kovalev et al., 2014) and for the Medicina Radio Telescope we estimate the correlated flux density to be ~60 mJy.

In order to calculate size and brightness temperature of the compact core feature, one needs to know its total flux density at the so-called “zero” spacing. The core flux density of 320 mJy is estimated from modeling the 2.3 GHz imaging data obtained in June 2014 during the VLBA calibrator survey campaign (VCS-II) (Gordon et al., 2016) assuming that the flux density did not change significantly over the year since the VLBA observations and the spectrum is flat. This is supported by comparing visibility data with our measurements within *RadioAstron* observations of TXS 0506+056 at similar ground baselines at 1.7 and 4.8 GHz. Using the core total flux density and correlated flux density at space-ground baseline and assuming a circu-

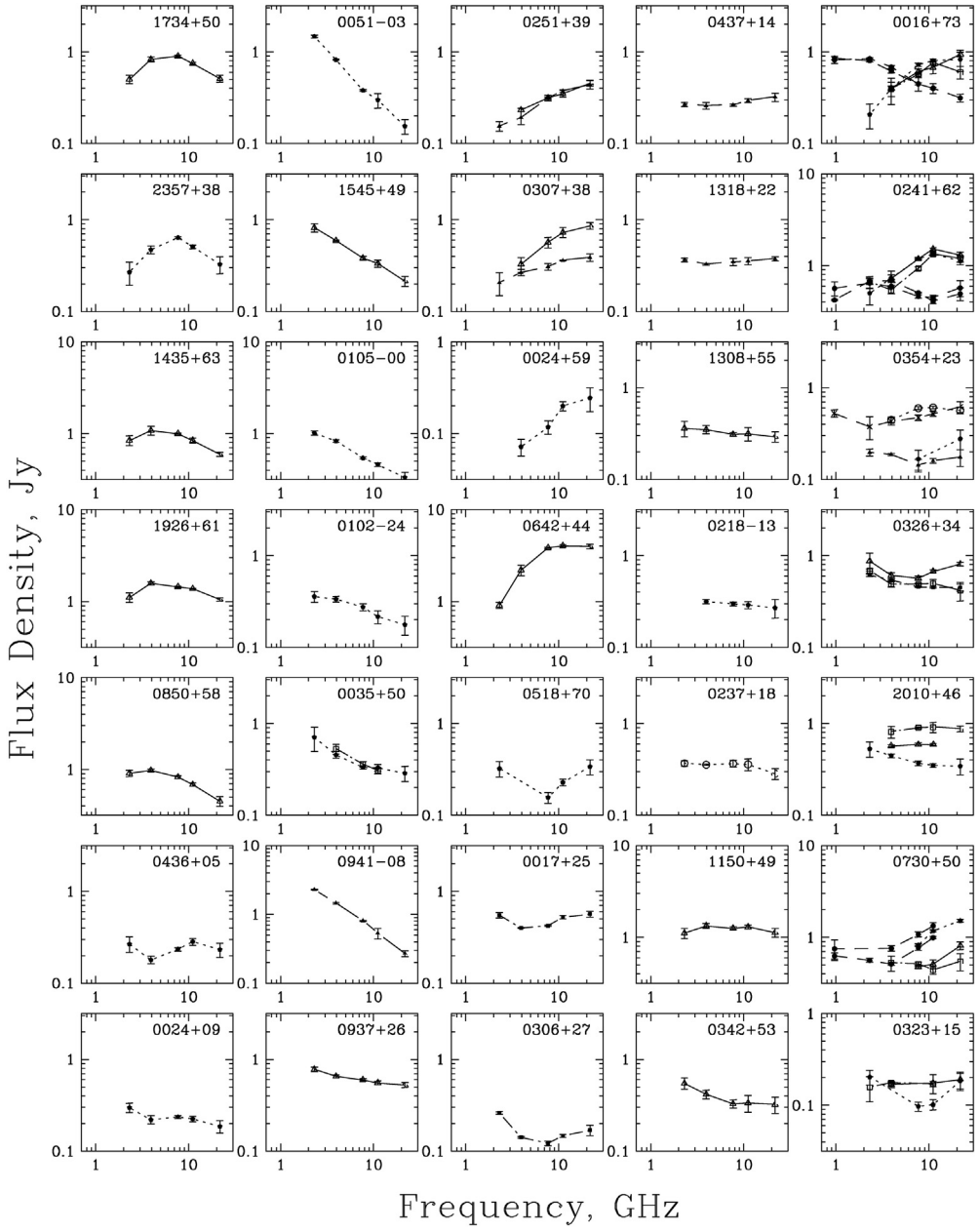

Fig. 4. Examples of five spectral types for the instantaneous spectra found among the 2600 observed AGN (left to right columns): (1) peaked (11%), (2) steep (the spectral indices $\alpha < -0.1$ in $F_\nu \propto \nu^\alpha$, – 41%), (3) inverted ($\alpha > +0.1$ at 3 or more the highest frequencies, – 10%), (4) super-flat ($|\alpha| \leqslant 0.1$ at 3 or more the highest frequencies, – 20%), (5) variable (changing between the above types 1–4, – 14%). The B1950 names of the objects are given in the boxes.

lar Gaussian brightness distribution we estimate the angular size (Lobanov, 2015) of the emitting region $\theta = 0.34$ mas, which corresponds to a linear size of $d = 1.6$ pc.

Following Kovalev et al. (2005), we obtain the corresponding brightness temperature in the source frame to be $T_b = 1.6 \times 10^{12}$ K, a factor of 2–5 above the MOJAVE VLBA measurements at 15 GHz reported by Kun et al. (2019). Our size and T_b estimates, in particular, show that the correlated flux density of TXS 0506+056 on projected baselines of >9 Earth diameters can be well below the *RadioAstron* detection level, which explains the absence of detections in other observations. We note that a lower limit of brightness temperature $T_{b,min}$ can be estimated directly from visibility amplitude measurements following the approach suggested by Lobanov (2015). This limit implies that the brightness temperature of the emission detected by the *RadioAstron* measurements cannot be smaller than $T_{b,min} = 1.3 \times 10^{12}$ K. The estimated T_b is in agreement with this limit.

According to the detection statistics of the *RadioAstron* AGN Survey (Kovalev et al., this issue), about (65–60)% of the objects observed at 1.7 and 4.8 GHz have been detected at 6 Earth diameters (ED) but the fraction of detected

Table 1
List of *RadioAstron* AGN survey observations of TXS 0506+056. The projected baseline length is shown in Earth diameters (ED). Telescope abbreviations: Ar = Arecibo 305 m, Gb = Green Bank 100 m, Ef = Effelsberg 100 m, Cd = Ceduna 30 m, Ev = Evpatoria 70 m, Hh = Hartebeesthoek 26 m, Kl = Kalyazin 64 m, Mc = Medicina 32 m, Nt = Noto 32 m, Ro = Robledo 70 m, Sv = Svetloe 32 m, Tr = Torun 32 m, Wb = Westerbork Synthesis Radio Telescope, Ys = Yebes 40 m, Zc = Zelenchukskaya 32 m.

Experiment	Observing	Ground telescopes		Baseline
code	epoch	1.7 GHz	4.8 GHz	ED
raks01by	2013 Sep 15	Tr, Wb	Ef, Ev, Mc, Ys	9.7
raks01cd	2013 Sep 16	Tr, Wb	Ef, Mc	13
raks01cg	2013 Sep 17	Ro, Tr	Ev, Ys	15
raks01ci	2013 Sep 17	Ar	Ar	16
raks01cl	2013 Sep 18	Gb, Kl, Zc	Gb, Sv	17
raks01cv	2013 Sep 24	Tr, Wb, Zc	Ef, Nt, Ys	11
raks01eh	2013 Oct 05	Ev, Nt, Ro	Ev, Ys	16
raks01es	2013 Oct 10	Zc	Sv, Ys	9.0
raks01qg	2014 Jan 12	Hh, Kl, Mc, Ro	Hh, Kl, Tr, Ys	11
raks01sn	2014 Jan 31	Ef, Tr	Tr, Ys	14
raks08bd	2014 Sep 19	Wb	Wb	14
raks08bm	2014 Sep 26	Gb, Hh, Kl, Sv	Hh, Kl, Zc	11
raks12cd	2015 Sep 23	Cd, Mc	Nt, Tr, Ys	5.9

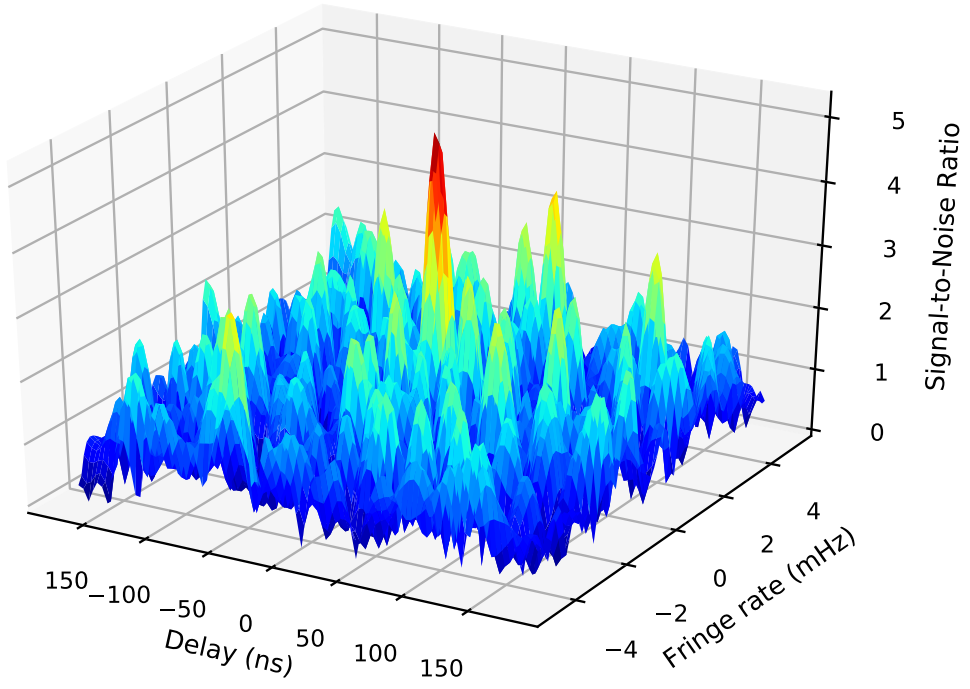

Fig. 5. *RadioAstron* (Space Radio Telescope–Medicina) 1.7 GHz interferometer response from observation of TXS 0506+056 on September 23, 2015 with a projected baseline of 414 Mλ (5.9 Earth diameters). The ratio of the interferometer fringe amplitude to the average noise amplitude is plotted as a function of the residual delay (in nanoseconds) and fringe rate (in millihertz). The signal-to-noise ratio is 5.5. The signal flux density is estimated by 60 mJy. The probability of false detection is estimated to be less than 5%.

sources are decreased to (45–40)% at 9 ED and to (15–10)% at 17 ED.

The *RadioAstron* non-detections at 1.7 and 4.8 GHz in 2014–2015 may also be understood by decomposing the 1–22 GHz spectra of TXS 0506+056 in Fig. 1 during the time of observations into the LFC and the HFC as:

$$F_{LFC} \simeq 0.53\ \nu^{-0.7} \quad (Jy), \tag{1}$$

$$F_{HFC} \simeq F_{tot} - F_{LFC} \quad (Jy). \tag{2}$$

Here the flux densities F_{LFC}, F_{HFC} and F_{tot} (all in Jy) are estimated at the frequency ν (in GHz). We use the rough estimations for the non-variable extended LFC as the minimal level of the observed flux density equal to 0.53 Jy during 20 years at 1 GHz as well as for the spectral index equal to 0.7 as the known typical index for the mean spectra of extra-galactic radio sources. As a result we have $F_{tot} \approx (0.4 \div 0.5)$ Jy, $F_{LFC} \simeq 0.37$ Jy, $F_{HFC} \simeq (0.03 \div 0.13)$ Jy at 18 cm; $F_{tot} \approx (0.40 \div 0.55)$ Jy, $F_{LFC} \simeq 0.18$ Jy, $F_{HFC} \simeq (0.22 \div 0.37)$ Jy at 6.2 cm. These low flux density

levels are consistent with the *RadioAstron* non-detections taking into consideration the non-detection statistics (Kovalev et al., this issue), the full resolution of the extended LFC and the possible partial resolution of the compact HFC on space-ground baselines.

Further, from (1) and (2) we obtain $F_{LFC} \simeq 0.08$ Jy and $F_{HFC} \simeq (0.32 \div 0.37)$ Jy in 2015–2016 and $F_{HFC} \simeq (0.55 \div 0.82)$ Jy in 2017–2018 at 15 GHz. These are in agreement with the MOJAVE correlated 15 GHz flux density of ~ 0.7 Jy measured on 2018 May 31 on long VLBA baselines and attributed to the core (Kun et al., 2019).

New *RadioAstron* observations of this source are scheduled between September 2018 and March 2019. Using the RATAN-600 observations in May–June 2018, we estimate the following flux densities for *RadioAstron* from the flat-spectrum flux densities $F_{tot} \approx 0.8$ Jy: $F_{HFC} \simeq 0.8 - 0.37 \simeq 0.4$ Jy at 18 cm, $F_{HFC} \simeq 0.8 - 0.18 \simeq 0.6$ Jy at 6 cm and $F_{HFC} \simeq 0.8 - 0.06 \simeq 0.7$ Jy at 1.35 cm. Such values could give positive detections with *RadioAstron* if the radio emitting region is sufficiently small. We note that there is no one-to-one correlation between a *RadioAstron* detection and an activity state of a radio source (Edwards et al., this issue).

4. Discussion

There are two main regions in AGN where the acceleration of particles may take place: near the super-massive black hole (SMBH) and in the jet. High energy protons and neutrinos may be generated around a SMBH in the central region (the core) of AGN and escape quasi-isotropically. Then relativistic protons at lower energies together with electrons are taken by the magnetic field of a core and may form the compact narrow jet in the longitudinal magnetic field near the magnetic poles. The particles move along the jet to a relatively extended periphery of the AGN and emit by the synchrotron mechanism. The emission along the jet is variable if the ejecting flow of protons from the core is variable, but it will be constant if the flow is steady at the start of the jet over a long time (Figs. 5 and 2 and Eqs. (1)–(6) in Kovalev et al., 2000a). This emission forms the observed High Frequency Component (HFC) of the radio spectrum. The magnetized periphery collects the matter from the jet. Synchrotron emission from particles in the tangled magnetic field very slowly increases with the age of the object and forms the observed quasi-stable Low Frequency Component (LFC) (Kovalev and Kovalev, 1998, 1999). The instantaneous spectra in Figs. 1, 2, and 4 are similar to the one- and two-component spectra calculated in the jet model with the longitudinal magnetic field of Figs. 2 and 5 in Kovalev et al. (2000a).

In Appendix A we have summarized from the literature some results on cosmic rays, neutrinos and protons which may be useful for understanding the new possible role of protons – both in producing the high-energy extragalactic neutrinos and in generating of the radio and HF-emission of jets in AGN. So, one can assume that the blazar TXS 0506+056 and other AGN may be associated with relativistic protons, which are necessary to produce the high-energy neutrino (e.g. Mészáros, 2017) and may also contribute to the radio emission.

Nevertheless, one can ask: why has proton-synchrotron emission not previously been considered in extragalactic astrophysics? The answer is simple: because of the absence of very strong arguments in favour of relativistic protons.

We now have at least two arguments: the discovery of high-energy neutrinos associated with this AGN by the IceCube Observatory as well as the *RadioAstron* detection of a bright core in this AGN with brightness temperature of more than 10^{12} K. Generation of relativistic protons with energies higher than 10^9 – 10^{10} eV in the nucleus of this AGN might explain both results. This might actually be a common phenomenon in AGN which could explain both the extragalactic neutrinos (IceCube) and extreme brightness temperatures found in many AGN (Kovalev et al., this issue).

The neutrino emitter TXS 0506+056 is unremarkable among other BL Lacs and among other AGN with variable radio emission. This might be a sign that either neutrino emission is common only among BL Lac objects, or among BL Lacs with the super-flat spectra or, among all AGN. In fact, TXS 0506+056 is not a unique high-energy neutrino emitter. Another similar AGN (although not at 3 sigma confidence) is PKS 0723−008. Its variable spectrum is shown at Fig. 2. Its spectral type is variable between the 'super-flat' and 'peaked'. TXS 0506+056 may also be a quasar. So, it is more likely that the neutrino emission is common among all AGN. The analysis by Kovalev et al. (2002b) has also shown that the observed main features of the broad-band radio spectra are similar for the main populations of 660 compact extragalactic source (AGN) – quasars, galaxies, blazars, γ-ray sources (EGRET detected), and highly polarized objects. The suggested jet models are also not specific to different types of AGN. Hence it follows that TXS 0506+056 and all other AGN could really produce relativistic protons and high-energy neutrinos as well as generate the proton-synchrotron emission in their jets.

While the common models of AGNs explain their emission, as a rule, by the synchrotron radiation of electrons, the proton-synchrotron radiation has been discussed in a number of studies. It was considered theoretically by Kardashev (2000), who showed that the proton-synchrotron radiation is characterized by the limiting intrinsic $T_b \sim 10^{16}$ K, while for the electron-synchrotron radiation the "Compton catastrophe" limits the intrinsic $T_b < 10^{12}$ K (Kellermann and Pauliny-Toth, 1969; Readhead, 1994). Consequently, the proton-synchrotron radiation was suggested as one of the possible mechanisms explaining extreme brightness temperatures observed by the ground and space VLBI (Kovalev et al., 2005; Gómez et al., 2016; Kovalev et al., 2016; Kardashev et al., 2017;

Kravchenko et al., 2020). The synchrotron emission of protons is used in modeling the spectral energy distributions of blazars in X-rays and gamma rays (Basumallick and Gupta, 2017a; Gao et al., 2018; Zhang et al., 2019). Proton-synchrotron radiation is also considered as the origin of X-rays and gamma rays from the extended (kpc-scale) jet of BL Lac type object AP Librae (Basumallick and Gupta, 2017b). Some results of synchrotron jet model simulations can be used both for electrons and protons (see Appendix A).

If the ongoing *RadioAstron* observations result in a detection on space-ground baselines, it may allow us to perform a detailed comparison of TXS 0506+056 to other blazars and AGN observed within the *RadioAstron* AGN survey in terms of the brightness temperature (T_b), radio core shape and size as a function of frequency as well as put constraints on the magnetic field strength in the cm-band core region. While for a given energy the synchrotron radiation of electrons (thanks to their lower mass) can outshine that of protons, the energy distribution of electrons and protons in the jet may differ due to a different balance between the acceleration and cooling.

One may compare the magnetic field H and the cooling time for a synchrotron source consisting of electrons and a similar source consisting of protons. From Ginzburg and Syrovatskii (1969), Pacholczyk (1970) we have

$$\nu \sim \nu_m = 0.29\,\frac{3eH_\perp}{4\pi\,Mc}\left(\frac{E}{Mc^2}\right)^2 = 1.2\cdot 10^6 H_\perp\left(\frac{E}{mc^2}\right)^2\,[\mathrm{Hz}] \propto \frac{H_\perp}{M}; \tag{3}$$

$$\frac{dE}{dt} = -\beta E^2, \quad E(t) = \frac{E_0}{1+\beta\,E_0\,t}, \quad \beta = \frac{2e^4 H_\perp}{3M^4c^7}; \tag{4}$$

$$T_{1/2} = \frac{1}{\beta E_0} = \frac{3M^3c^5}{2e^4H_\perp^2}\left(\frac{M\,c^2}{E_0}\right) = \frac{5.1\cdot 10^8}{H_\perp^2}\left(\frac{mc^2}{E_0}\right)\,[s] \propto \frac{M^3}{H_\perp^2}. \tag{5}$$

Here ν and ν_m are an observed frequency and the frequency of the maximum in the spectra of synchrotron emission of the particle (an electron or a proton); M is the mass of the particle; $H_\perp \equiv H\sin\psi$, where ψ is the pitch-angle; $T_{1/2}$ is the cooling time at which the initial energy E_0 of the particle is decreased by a factor of 2 because of the synchrotron emission. The numeric terms in Eqs. (3) and (5) are shown for electrons.

In addition, we suggest that $\nu^{(e)} = \nu^{(p)}$ as well as $(E/Mc^2)_p = (E/mc^2)_e \geqslant 10$ where the subscripts or superscripts (e) and (p) are used to signify the parameters for electrons and protons, respectively. If the emitted radio spectrum, the value of (E/Mc^2) and the distribution of pitch-angles are also the same for electrons and protons then we obtain from (3)–(5)

$$H_\perp^{(p)}/H_\perp^{(e)} = M_p/m_e \sim 2000, \tag{6}$$

$$T_{1/2}^{(p)}/T_{1/2}^{(e)} = M_p/m_e \sim 2000. \tag{7}$$

So, if we substitute electrons by protons under the conditions above, the presumed typical magnetic field $H_\perp^{(e)} \sim 1$ Gauss in an electron synchrotron source has to be changed to $H_\perp^{(p)} \sim 2000$ Gauss in the similar proton-synchrotron source. The cooling time for electrons $T_{1/2}^{(e)} \leqslant 1.6$ years in this field will change to $T_{1/2}^{(p)} \leqslant 3200$ years for protons if $(mc^2/E_0) \leqslant 0.1$ ($\nu = \nu^{(e)} = \nu^{(p)} \geqslant 1.2\cdot 10^8$ Hz).

The spectra of an electron and proton-dominated synchrotron sources may look alike, but the physical conditions needed to produce them differ substantially. For a given fluence, the proton-synchrotron source would require a much stronger magnetic field and a way to suppress the synchrotron radiation of electrons. The latter may be achieved if the particle acceleration mechanism (balanced by cooling) is considerably more efficient for protons rather than electrons. One substantial difference between the electron and proton-dominated synchrotron sources is the cooling time. The cooling time may be related to a variability timescale at a given frequency. However, despite numerous attempts, no blazar variability feature at any wavelength has been unambiguously linked to the cooling time, so using this difference to distinguish proton from synchrotron blazars would not be straightforward before a detailed model analysis.

It is also perfectly possible that the synchrotron radiation of protons is completely swamped by the synchrotron radiation of electrons in radio band. In this case we may hope to get indirect clues about the population of high-energy protons from radio observations: identify a flare that may be related to enhanced acceleration of protons (as well as the observed electrons). No such features could be identified yet. The ongoing flare of TXS 0506+056 is comparable to the one experienced by the source in 2005–2009 (IceCube observations started in April 2008, Aartsen et al. (2018b)) and as the neutrino event IceCube-170922A was detected on the rising part of the flare after a deep minimum, the cm-band radio flux level at that time was actually close to the average level observed by RATAN-600 over the past 20 years (Fig. 3). The low-energy neutrino events reported by Aartsen et al. (2018b) correspond to the low level of activity in the radio band. The low level of activity at that time was reported also at GeV γ-rays and other bands by Padovani et al., 2018 which poses a challenge to the current neutrino-emission models (Rodrigues et al., 2019).

5. Summary

Twenty years of observational study of 1–22 GHz instantaneous spectra with the RATAN-600 and the first measurements with the *RadioAstron* Space VLBI of the high-energy neutrino emitter TXS 0506+056 have shown that it is a typical variable AGN with the 'super-flat' radio

spectrum – unremarkable among the several hundreds other monitored AGNs. *RadioAstron* Space VLBI observations estimate the observer's frame brightness temperature at an epoch prior to the neutrino detection at the level of about or greater than 10^{12} K. The observed properties of this object are consistent with both electron-synchrotron and proton-synchrotron emission. The synchrotron emitting protons are expected to have a much more stable energy distribution compared to electrons due to the longer proton cooling time. However, if both emission mechanisms are present in one source, the electron synchrotron emission may produce fast variability while the proton synchrotron may be responsible for the long-term variable emission. Future multi-wavelength and space VLBI observations may test this possibility. New *RadioAstron* observations are scheduled between September 2018 and March 2019.

Acknowledgements

We are grateful to two anonymous referees for useful comments which helped to improve the manuscript. This research is based on observations with RATAN-600 of the Special Astrophysical Observatory of the Russian Academy of Sciences. The *RadioAstron* project is led by the Astro Space Center of the Lebedev Physical Institute of the Russian Academy of Sciences and the Lavochkin Scientific and Production Association under a contract with the State Space Corporation ROSCOSMOS, in collaboration with partner organizations in Russia and other countries. The results are partly based on observations performed with radio telescopes of IAA RAS, the 100-m telescope of the MPIfR (Max-Planck-Institute for Radio Astronomy) at Effelsberg, the Medicina and Noto telescopes operated by INAF – Istituto di Radioastronomia, the DSS-63 antenna at the Madrid Deep Space Communication Complex under the Host Country Radio Astronomy program, the 40-m radio telescope of the National Geographic Institute of Spain (IGN) at Yebes Observatory. Partly based on the Evpatoria RT-70 radio telescope (Ukraine) observations carried out by the Institute of Radio Astronomy of the National Academy of Sciences of Ukraine under a contract with the State Space Agency of Ukraine and by the National Space Facilities Control and Test Center with technical support by Astro Space Center of Lebedev Physical Institute, Russian Academy of Sciences. This work is based in part on observations carried out using the 32-m radio telescope operated by Torun Centre for Astronomy of Nicolaus Copernicus University in Torun (Poland) and supported by the Polish Ministry of Science and Higher Education SpUB grant. The Hartebeesthoek telescope is a facility of the National Research Foundation of South Africa. The Green Bank Observatory is a facility of the National Science Foundation operated under cooperative agreement by Associated Universities, Inc. The Arecibo Observatory is operated by SRI International under a cooperative agreement with the National Science Foundation (AST-1100968), and in alliance with Ana G. Mendez-Universidad Metropolitana, and the Universities Space Research Association. The Westerbork Synthesis Radio Telescope is operated by the ASTRON (Netherlands Foundation for Research in Astronomy) with support from the Netherlands Foundation for Scientific Research (NWO). Results of optical positioning measurements of the Spektr-R spacecraft by the global MASTER Robotic Net (Lipunov et al., 2010), ISON collaboration, and Kourovka observatory were used for spacecraft orbit determination in addition to mission facilities. This paper was supported in part by the government of the Russian Federation (agreement 05.Y09.21.0018) and the Alexander von Humboldt Foundation.

Appendix A. Cosmic rays, neutrinos, protons, jets in AGN

The IceCube project has discovered a flux of cosmic neutrinos in the high-energy range from 10^{13} to 10^{16} eV, predominantly extragalactic in origin, as well as neutrino emission from the direction of the blazar TXS 0506+056 prior to the IceCube-170922A alert. This suggests that blasars are the first identified sources of the high-energy astrophysical neutrino flux (Aartsen et al., 2018b; Ahlers and Halzen, 2018). Ahlers and Halzen (2018) conclude that "the corresponding energy density is close to that of ...ultra-high-energy cosmic rays observed with large surface detectors. Neutrinos are therefore ubiquitous in the nonthermal universe, suggesting a more significant role of protons (nuclei) relative to electrons than previously anticipated."

This may extend to a more significant role for relativistic protons relative to electrons in the synchrotron emission of jets in AGN than has previously been assumed. This allows to solve some old problems for physics of the jet models. In particular, to increase at ~ 2000 times the magnetic field of the jet and the cooling time thanks to emitted protons (see (6)–(7) above) as well as to give simple explanations for curve jets.

Moreover, it is possible to use some earlier results of analysis – e.g. by Kovalev et al. (2000a) – on fitting a jet model of AGN to instantaneous spectra observations of 34 AGN because these fits have been done relative to the normalized parameters of the model – without using the absolute values of the magnetic field and other parameters of the jet. A similar approach had been also used to the results of simulation in this model of flares observed in B 0235+16 over 1.5 years at eight frequencies from 0.3 to 15 GHz by Kovalev and Larionov (1994). For example, for the case of radio emission by relativistic electrons, it had been estimated the magnetic field $B_0 \sim 0.25$ G in this paper at the jet base. We would obtain $B_0 \sim 0.25 * 2000 = 500$ G if emit relativistic protons rather the electrons, and if all other the suggestions for (6)–(7) are satisfied.

References

Aartsen, M.G., Ackermann, M., et al.IceCube Collaboration, 2018a. Multimessenger observations of a flaring blazar coincident with high-energy neutrino IceCube-170922A. Science 361, eaat1378. https://doi.org/10.1126/science.aat1378, arXiv: 1807.08816.

Aartsen, M.G., Ackermann, M., et al.IceCube Collaboration, 2018b. Neutrino emission from the direction of the blazar TXS 0506+056 prior to the IceCube-170922A alert. Science 361, 147–151. https://doi.org/10.1126/science.aat2890, arXiv:1807.08794..

Aartsen, M.G., Ackermann, M., Adams, J., et al., 2017. The IceCube Neutrino Observatory: instrumentation and online systems. J. Instrum. 12, P03012. https://doi.org/10.1088/1748-0221/12/03/P03012, arXiv: 1612.05093.

Ackermann, M., Ajello, M., Atwood, W.B., et al., 2015. The third catalog of active galactic nuclei detected by the fermi large area telescope. ApJ 810, 14. https://doi.org/10.1088/0004-637X/810/1/14, arXiv:1501.06054..

Ahlers, M., Halzen, F., 2018. Opening a new window onto the universe with IceCube. Prog. Part. Nucl. Phys. 102, 73–88. https://doi.org/10.1016/j.ppnp.2018.05.001, arXiv: 1805.11112.

Aller, H.D., Aller, M.F., Latimer, G.E., Hodge, P.E., 1985. Spectra and linear polarizations of extragalactic variable sources at centimeter wavelengths. ApJS 59, 513–768. https://doi.org/10.1086/191083.

Angelakis, E., Fuhrmann, L., Myserlis, I., et al., 2019. F-GAMMA: Multi-frequency radio monitoring of Fermi blazars. The 2.64 to 43 GHz Effelsberg light curves from 2007–2015. arXiv e-prints doi: https://doi.org/10.1051/0004-6361/201834363, arXiv: 1902.04404.

Ansoldi, S., Antonelli, L.A., Arcaro, C., et al., 2018. The Blazar TXS 0506 +056 associated with a high-energy neutrino: insights into extragalactic jets and cosmic-ray acceleration. ApJL 863, 10. https://doi.org/10.3847/2041-8213/aad083, arXiv:1807.04300..

Basumallick, P.P., Gupta, N., 2017a. A single zone synchrotron model for flares of PKS1510-089. Astropart. Phys. 88, 1–6. https://doi.org/10.1016/j.astropartphys.2016.12.005, arXiv:1609.02370..

Basumallick, P.P., Gupta, N., 2017b. Constraints on a proton synchrotron origin of VHE gamma rays from the extended jet of AP librae. ApJ 844, 58. https://doi.org/10.3847/1538-4357/aa7a12, arXiv: 1706.04895.

Dodson, R., Fomalont, E.B., Wiik, K., et al., 2008. The VSOP 5 GHz active galactic nucleus survey. V. Imaging results for the remaining 140 sources. ApJS 175, 314–355. https://doi.org/10.1086/525025, arXiv:0710.5707.

Ehman, J.R., Dixon, R.S., Kraus, J.D., 1970. The Ohio survey between declinations of 0 and 36 south. AJ 75, 351–506. https://doi.org/10.1086/110985.

Gao, Q.G., Lu, F.W., Ma, J., Ren, J.Y., Li, H.Z., 2018. Is the GeV-TeV emission of PKS 0447–439 from the proton synchrotron radiation? Ap&SS 363, 119. https://doi.org/10.1007/s10509-018-3341-y.

Ginzburg, V.L., Syrovatskii, S.I., 1969. Developments in the theory of synchrotron radiation and its reabsorption. ARA&A 7, 375–420. https://doi.org/10.1146/annurev.aa.07.090169.002111.

Giovannini, G., Savolainen, T., Orienti, M., et al., 2018. A wide and collimated radio jet in 3C84 on the scale of a few hundred gravitational radii. Nat. Astron. 2, 472–477. https://doi.org/10.1038/s41550-018-0431-2, arXiv:1804.02198..

Gómez, J.L., Lobanov, A.P., Bruni, G., et al., 2016. Probing the innermost regions of AGN jets and their magnetic fields with radio astron. I. Imaging BL lacertae at 21 microarcsecond resolution. ApJ 817, 96. https://doi.org/10.3847/0004-637X/817/2/96, arXiv: 1512.04690.

Gordon, D., Jacobs, C., Beasley, A., et al., 2016. Second epoch VLBA calibrator survey observations: VCS-II. AJ 151, 154. https://doi.org/10.3847/0004-6256/151/6/154.

Gorshkov, A.G., Konnikova, V.K., 1996. Rapid variability of extragalactic radio sources at centimeter wavelengths. Astron. Rep. 40, 314–318.

Halzen, F., 2016. IceCube and the discovery of high-energy cosmic neutrinos. Int. J. Modern Phys. D 25, 1630028–1631510. https://doi.org/10.1142/S0218271816300287.

Hirabayashi, H., Fomalont, E.B., Horiuchi, S., et al., 2000. The VSOP 5 GHz AGN survey I. Compilation and observations. PASJ 52, 997–1014. https://doi.org/10.1093/pasj/52.6.997.

Kardashev, N.S., 2000. Radio synchrotron emission by protons and electrons in pulsars and the nuclei of quasars. Astron. Rep. 44, 719–724. https://doi.org/10.1134/1.1320497.

Kardashev, N.S., Khartov, V.V., Abramov, V.V., et al., 2013. "Radio-Astron"-A telescope with a size of 300 000 km: main parameters and first observational results. Astron. Rep. 57, 153–194. https://doi.org/10.1134/S1063772913030025, arXiv:1303.5013.

Kardashev, N.S., Alakoz, A.V., Andrianov, A.S., et al., 2017. Radio-Astron science program five years after launch: main science results. Sol. Syst. Res. 51, 535–554. https://doi.org/10.1134/S0038094617070085.

Kellermann, K.I., Pauliny-Toth, I.I.K., 1969. The spectra of opaque radio sources. ApJL 155, L71–L78. https://doi.org/10.1086/180305.

Korolkov, D.V., Pariiskii, I.N., 1979. The Soviet RATAN-600 radio telescope. S&T 57, 324–329.

Kovalev, Y.A., Kovalev, Y.Y., 1998. Do jets exist in all compact extragalactic objects?. In: Zensus, J.A., Taylor, G.B., Wrobel, J.M. (Eds.), IAU Colloq. 164: Radio Emission from Galactic and Extragalactic Compact Sources, ASP Conf. Ser. 144. ASP, San Francisco, pp. 275–276.

Kovalev, Y.A., Kovalev, Y.Y., 1999. On the nature of radio emission of AGNs: spectra, milli-arcsecond structure and polarization. In: Terzian, Y., Khachikian, E., Weedman, D. (Eds.), Activity in Galaxies and Related Phenomena. ASP, San Francisco, pp. 82–83.

Kovalev, Y.Y., Larionov, G.M., 1994. The search for variable quasars and galaxies suitable for cosmological radio measurements: quasar 0235+16. Astron. Lett. 20, 3–7.

Kovalev, Y.Y., Nizhelsky, N.A., Kovalev, Y.A., et al., 1999. Survey of instantaneous 1–22 GHz spectra of 550 compact extragalactic objects with declinations from -30° to +43°. A&AS 139, 545–554. https://doi.org/10.1051/aas:1999406, arXiv:astro-ph/0408264.

Kovalev, Y.A., Kovalev, Y.Y., Nizhelsky, N.A., 2000a. Broad-band spectra study of 213 VSOP 5-GHz survey sources. PASJ 52, 1027–1036. https://doi.org/10.1093/pasj/52.6.1027.

Kovalev, Y.A., Kovalev, Y.Y., Nizhelsky, N.A., 2000b. Instantaneous 1–22 GHz spectra of 214 VSOP survey sources. In: Hirabayashi, H., Edwards, P.G., Murphy, D.W. (Eds.), Astrophysical Phenomena Revealed by Space VLBI. Institute of Space and astronautical Science, Sagamihara, Kanagawa, pp. 193–198.

Kovalev, Y.Y., Kovalev, Y.A., Nizhelsky, N.A., Bogdantsov, A.B., 2002a. Broad-band radio spectra variability of 550 AGN in 1997–2001. PASA 19, 83–87. https://doi.org/10.1071/AS01109.

Kovalev, Y.Y., Nizhelsky, N.A., Kovalev, Y.A., Zhekanis, G.V., Bogdantsov, A.V., 2002b. Survey and Analysis of 1–22 GHz Spectra for the Full Sample of 660 AGNs North of Declination -30 Degrees. In: Green, R.F., Khachikian, E.Y., Sanders, D.B. (Eds.), IAU Colloq. 184: AGN Surveys, ASP Conf. Ser. 284. ASP: San Francisco, pp. 299–300.

Kovalev, Y.Y., Kovalev, Y.A., Nizhelsky, N.A., Zhekanis, G.V., 2004. Types and structure of instantaneous spectra for 2600 extragalactic VLBI objects on the data of 5–6 frequencies from 1 to 22 GHz with the RATAN-600 (in Russian). Trans. Sternberg Astron. Inst. 75, 116.

Kovalev, Y.Y., Kellermann, K.I., Lister, M.L., et al., 2005. Sub-milliarcsecond imaging of quasars and active galactic nuclei. IV. Fine-scale structure. AJ 130, 2473–2505. https://doi.org/10.1086/497430, arXiv: astro-ph/0505536.

Kovalev, Y.A., Vasil'kov, V.I., Popov, M.V., et al., 2014. The Radio-Astron project: measurements and analysis of basic parameters of space telescope in flight in 2011–2013. Cosm. Res. 52, 393–402. https://doi.org/10.1134/S0010952514050074.

Kovalev, Y.Y., Kardashev, N.S., Kellermann, K.I., et al., 2016. Radio-Astron observations of the quasar 3C273: a challenge to the brightness

temperature limit. ApJL 820, L9. https://doi.org/10.3847/2041-8205/820/1/L9, arXiv:1601.05806.

Kravchenko, E.V., Gómez, J.L., Kovalev, Y.Y., Voytsik, P.A., 2020. The jet of S5 0716+71 at μas scales with RadioAstron. Adv. Space Res., 65 (2), 720–724.

Kun, E., Biermann, P.L., Gergely, L.Á., 2019. Very long baseline interferometry radio structure and radio brightening of the high-energy neutrino emitting blazar TXS 0506+056. MNRAS 483, L42–L46. https://doi.org/10.1093/mnrasl/sly216, arXiv: 1807.07942.

Kutkin, A.M., Pashchenko, I.N., Lisakov, M.M., et al., 2018. The extreme blazar AO 0235+164 as seen by extensive ground and space radio observations. MNRAS 475, 4994–5009. https://doi.org/10.1093/mnras/sty144, arXiv: 1801.04892.

Likhachev, S.F., Kostenko, V.I., Girin, I.A., et al., 2017. Software correlator for radioastron mission. J. Astron. Instrument. 6, 1750004–1750131. https://doi.org/10.1142/S2251171717500040, arXiv: 1706.06320.

Lipunov, V., Kornilov, V., Gorbovskoy, E., et al., 2010. Master robotic net. Adv. Astron. 2010, 349171. https://doi.org/10.1155/2010/349171, arXiv: 0907.0827.

Lobanov, A., 2015. Brightness temperature constraints from interferometric visibilities. A&A 574, A84. https://doi.org/10.1051/0004-6361/201425084, arXiv: 1412.2121.

Mannheim, K., 1995. High-energy neutrinos from extragalactic jets. Astropart. Phys. 3, 295–302. https://doi.org/10.1016/0927-6505(94)00044-4.

Mészáros, P., 2017. Astrophysical sources of high-energy neutrinos in the IceCube era. Annu. Rev. Nucl. Part. Sci. 67, 45–67. https://doi.org/10.1146/annurev-nucl-101916-123304, arXiv: 1708.03577.

Mingaliev, M.G., Sotnikova, Y.V., Udovitskiy, R.Y., et al., 2014. RATAN-600 multi-frequency data for the BL Lacertae objects. A&A 572, A59. https://doi.org/10.1051/0004-6361/201424437, arXiv:1410.2835.

Pacholczyk, A.G., 1970. Radio Astrophysics: Nonthermal Processes in Galactic and Extragalactic Sources. Astronomy and Astrophysics Series. W.H. Freeman, San Francisco.

Padovani, P., Giommi, P., Resconi, E., et al., 2018. Dissecting the region around IceCube-170922A: the blazar TXS 0506+056 as the first cosmic neutrino source. MNRAS 480, 192–203. https://doi.org/10.1093/mnras/sty1852, arXiv: 1807.04461.

Padovani, P., Oikonomou, F., Petropoulou, M., Giommi, P., Resconi, E., 2019. TXS 0506+056, the first cosmic neutrino source, is not a BL Lac. MNRAS 484, L104–L108. https://doi.org/10.1093/mnrasl/slz011, arXiv: 1901.06998.

Paiano, S., Falomo, R., Treves, A., Scarpa, R., 2018. The Redshift of the BL Lac Object TXS 0506+056. ApJL 854, L32. https://doi.org/10.3847/2041-8213/aaad5e, arXiv: 1802.01939.

Petrov, L., Kovalev, Y.Y., Fomalont, E.B., Gordon, D., 2011. The very long baseline array galactic plane survey – VGaPS. AJ 142, 35. https://doi.org/10.1088/0004-6256/142/2/35, arXiv: 1101.1460.

Pilipenko, S.V., Kovalev, Y.Y., Andrianov, A.S., et al., 2018. The high brightness temperature of B0529+483 revealed by RadioAstron and implications for interstellar scattering. MNRAS 474, 3523–3534. https://doi.org/10.1093/mnras/stx2991, arXiv: 1711.06713.

Readhead, A.C.S., 1994. Equipartition brightness temperature and the inverse Compton catastrophe. ApJ 426, 51–59. https://doi.org/10.1086/174038.

Richards, J.L., Max-Moerbeck, W., Pavlidou, V., et al., 2011. Blazars in the Fermi Era: the OVRO 40 m telescope monitoring program. ApJS 194, 29. https://doi.org/10.1088/0067-0049/194/2/29, arXiv: 1011.3111.

Rodrigues, X., Gao, S., Fedynitch, A., Palladino, A., Winter, W., 2019. Leptohadronic blazar models applied to the 2014–2015 flare of TXS 0506+056. ApJL 874, L29. https://doi.org/10.3847/2041-8213/ab1267, arXiv: 1812.05939.

Slish, V.I., 1963. Angular size of radio stars. Nature 199, 682. https://doi.org/10.1038/199682a0.

Teräsranta, H., Wiren, S., Koivisto, P., Saarinen, V., Hovatta, T., 2005. 24 year monitoring of extragalactic sources at 22 and 37 GHz. A&A 440, 409–410. https://doi.org/10.1051/0004-6361:20053356.

Véron-Cetty, M.P., Véron, P., 2010. A catalogue of quasars and active nuclei: 13th edition. A&A 518, A10. https://doi.org/10.1051/0004-6361/201014188.

Zhang, H., Fang, K., Li, H., et al., 2019. Probing the Emission Mechanism and Magnetic Field of Neutrino Blazars with Multi-Wavelength Polarization Signatures. arXiv e-prints arXiv: 1903.01956.